

Electronic Supplementary Information for
A Molecular Structural Analog of Proposed Dinuclear Active Sites in Cobalt-
Based Water Oxidation Catalysts

Timothy C. Davenport, Hyun S. Ahn, Micah S. Ziegler, and T. Don Tilley*^a

^a Department of Chemistry, University of California, Berkeley, Berkeley, CA 94720-1460, USA
and Chemical Sciences Division, Lawrence Berkeley National Laboratory, Berkeley, CA 94720, USA.
E-mail: tdtilley@berkeley.edu

1. Experimental Details

2. X-ray crystallography Details

Table S1. Experimental details for the X-ray crystal structures of DPMN, DPFN, **1**, and **2**.

Figure S1. Crystal structure of DPMN.

Figure S2. Crystal structure of DPFN.

3. Computational Details

Figure S3. Optimized atomic coordinates of **1**.

Table S2. Cartesian coordinates of the optimized geometry of **1**.

Figure S4. Optimized atomic coordinates of $[\text{Co}^{\text{III}}(\text{OH}_2)\text{Co}^{\text{III}}(\text{OH})]$.

Table S3. Cartesian coordinates of the optimized geometry of $[\text{Co}^{\text{III}}(\text{OH}_2)\text{Co}^{\text{III}}(\text{OH})]$.

Figure S5. Optimized atomic coordinates of $[\text{Co}^{\text{III}}(\text{OH})]_2$.

Table S4. Cartesian coordinates of the optimized geometry of $[\text{Co}^{\text{III}}(\text{OH})]_2$.

Figure S6. Optimized atomic coordinates of $[\text{Co}^{\text{III}}(\text{OH}_2)\text{Co}^{\text{IV}}(\text{O})]$.

Table S5. Cartesian coordinates of the optimized geometry of $[\text{Co}^{\text{III}}(\text{OH}_2)\text{Co}^{\text{IV}}(\text{O})]$.

Figure S7. Optimized atomic coordinates of $[\text{Co}^{\text{III}}(\text{OH})\text{Co}^{\text{IV}}(\text{O})]$.

Table S6. Cartesian coordinates of the optimized geometry of $[\text{Co}^{\text{III}}(\text{OH})\text{Co}^{\text{IV}}(\text{O})]$.

Figure S8. Optimized atomic coordinates of $[\text{Co}^{\text{III}}]_2(\mu\text{-OOH})$.

Table S7. Cartesian coordinates of the optimized geometry of $[\text{Co}^{\text{III}}]_2(\mu\text{-OOH})$.

Table S8. Optimized Spin States for Computational Structures

4. Electrochemical Details

Figure S9. Cyclic voltammogram of 2 mM **1** at pH 9.0 in 0.1 M KP_i aqueous buffer solution and buffer only.

Figure S10. Cyclic voltammogram of 2 mM DPFN in 0.1 M ^tBu₄NPF₆ DMF solution.

Figure S11. Pourbaix diagram of **1** in phosphate buffer solution from pH 1–12 in the potential window 0–1.8 V vs. NHE.

Figure S12. Cathodic differential pulse voltammograms of **1** with variation of pH from 1.4–6.5.

Figure S13. Controlled potential electrolysis of **1** at 1.6 V in phosphate buffer solution at pH 9.0.

Figure S14. Evolved oxygen detection during controlled potential electrolysis.

Figure S15. Comparison of background-subtracted controlled potential electrolysis of **1** at 1.6 V in phosphate and borate buffer solutions at pH 9.

5. References

1. Experimental Details

General Considerations. Solvents were purchased from Aldrich at spectroscopic grade. For synthesis purposes, distilled, deionized water was used. Deuterated solvents were purchased from Cambridge Isotope Laboratories and used as received. *n*-Butyllithium, Co(NO₃)·6(H₂O), and 1-Chloromethyl-4-fluoro-1,4-diazoaniabicyclo[2.2.2]octane bis(tetrafluoroborate) (SelectFluor) were purchased from Aldrich and used as received. The reagents 1,1-di-(2-pyridyl)methane and 2,7-dichloro-1,8-naphthyridine were prepared according to literature procedures.^{18,1} NMR spectra were recorded on Bruker AV-600, AVQ-400 and AV-300 spectrometers at room temperature. ¹H NMR spectra were referenced to residual protio solvent peaks (δ 7.24 for *d*-chloroform, δ 5.32 for *d*₂-dichloromethane, δ 4.80 for *d*₂-water). ¹³C{¹H} NMR spectra were referenced to solvent resonances (δ 77.23 for *d*-chloroform, δ 54.00 for *d*₂-dichloromethane). Elemental analyses were carried out by the College of Chemistry Microanalytical Laboratory at the University of California, Berkeley. UV-Vis spectra were recorded on a Varian-Cary 300 Bio spectrophotometer at 1 nm resolution. Potentiometric titrations were performed using a Thermo Fisher Orion 3-Star pH meter with a Ag/AgCl combination pH electrode. Measurement of acid dissociation constants were not corrected for ionic strength.

Synthesis of 2,7-bis(di(2-pyridyl)methyl)-1,8-naphthyridine (DPMN). *n*-Butyllithium (1.6 M in hexanes, 125 mL, 200 mmol) was added dropwise to a stirred solution of freshly distilled 1,1-di-(2-pyridyl)methane (34.0 g, 200 mmol) in 400 mL of THF at 0° C under a N₂ atmosphere. The red solution was stirred for 30 min. after which 2,7-dichloro-1,8-naphthyridine (17.3 g, 87 mmol) was added. The purple solution formed was stirred for 16 h as the vessel warmed to room temperature. After addition of 50 mL of water, the mixture was filtered. The orange precipitate

was dissolved in a 1:1 CH₂Cl₂:H₂O mixture and filtered to remove residual 2,7-dichloro-1,8-naphthyridine. The organic fraction was washed with H₂O (2 x 100 mL) and then dried over MgSO₄ and evaporated to dryness. The crude material was crystallized from hot acetonitrile to give light orange crystals of 2,7-bis(1,1-di-(2-pyridyl)methyl)-1,8-naphthyridine (DPMN) (yield: 9.0 g, 19 mmol, 22%). Additional crystallizations from hot ACN (2 times) was performed to prepare light orange X-ray quality crystals. **¹H NMR** (*d*₂-dichloromethane, 600.13 MHz): δ 8.53 (d, *J*_{HH} = 4.1 Hz, of d, *J*_{HH} = 1.7 Hz, d, *J*_{HH} = 0.9 Hz, 4H), 8.10 (d, *J*_{HH} = 8.4 Hz, 2H), 7.65 (t, *J*_{HH} = 7.7 Hz, of d, *J*_{HH} = 1.9 Hz, 4H), 7.60 (d, *J*_{HH} = 8.4 Hz, 2H), 7.37 (d, *J*_{HH} = 7.9 Hz, 4H), 7.17 (d, *J*_{HH} = 7.4 Hz, of d, *J*_{HH} = 4.9 Hz, of d, *J*_{HH} = 0.9 Hz, 4H), 6.16 (s, 2H). **¹³C{¹H} NMR** (*d*₂-dichloromethane, 150.92 MHz): δ 165.6, 161.4, 155.8, 149.9, 137.3, 137.0, 124.9, 123.9, 122.4, 120.7, 65.4). **EA** Anal. Calcd (%) for C₃₀H₂₂N₆ (466.55): C, 77.23; H, 4.75; N, 18.01. Found: C, 77.55; H, 4.70; N, 17.85.

Synthesis of 2,7-bis(fluorodi(2-pyridyl)methyl)-1,8-naphthyridine (DPFN). SelectFluor (10.2 g, 29 mmol) was dissolved in 175 mL of ACN. DPMN (6.7 g, 14 mmol) was added and the mixture was refluxed for 16 hrs during which the DPMN dissolved. To the solution was added 75 mL of CH₂Cl₂ and 75 mL of H₂O. The organic phase was washed with H₂O (2 x 50 mL) and then dried over MgSO₄ and evaporated to dryness leaving a yellow solid. The product was purified by crystallization from slow cooling of a hot ACN solution as pale yellow crystals (2.8 g, 5.6 mmol, 39%). Further crystallization from hot ACN (2 times) was performed to prepare analytically pure colorless material and X-ray quality crystals. **¹H NMR** (*d*₂-dichloromethane, 300.13 MHz): δ 8.56 (d, *J*_{HH} = 4.5 Hz, 4H), 8.25 (d, *J*_{HH} = 8.7 Hz, 2H), 7.82 (d, *J*_{HH} = 8.4 Hz, 2H), 7.77 (t, *J*_{HH} = 8.1 Hz, of d, *J*_{HH} = 1.5 Hz, 4H), 7.58 (d, *J*_{HH} = 7.8 Hz, 4H), 7.29 (t, *J*_{HH} = 4.8 Hz, of d, *J*_{HH} = 1.5 Hz, 4H). **¹³C{¹H} NMR** (*d*₂-dichloromethane, 100.62 MHz): δ 164.2 (d, ²*J*_{CF}

$= 25$ Hz), 159.9 (d, ${}^2J_{\text{CF}} = 25$ Hz), 154.1, 149.3, 137.6, 137.2, 123.8, 123.1 (d, ${}^3J_{\text{CF}} = 6$ Hz), 122.3 (d, ${}^3J_{\text{CF}} = 5$ Hz), 121.8, 100.8 (d, ${}^1J_{\text{CF}} = 179$ Hz)). **${}^{19}\text{F}\{{}^1\text{H}\}$ NMR** (d_2 -dichloromethane, 376.48 MHz): $\delta -142.1$. **EA** Anal. Calcd (%) for $\text{C}_{30}\text{H}_{20}\text{F}_2\text{N}_6$ (502.52): C, 71.70; H, 4.01; N, 16.72. Found: C, 71.53; H, 4.15; N, 16.64. **UV/Vis** (acetonitrile, λ [nm] (ϵ [$\text{M}^{-1}\cdot\text{cm}^{-1} \div 10^3$])): 214 (82.5 ± 9.0), 255 (17.6 ± 1.8), 259 (17.8 ± 1.8), 308 (9.6 ± 0.97), 315 (10.2 ± 1.0).

Synthesis of $[\text{Co}_2(\mu\text{-OH})_2(\text{OH}_2)_2(\text{DPFN})][\text{NO}_3]_4$ (1). DPFN (0.3 g, 0.6 mmol) was dissolved with heating in 120 mL of EtOH to which was added a solution of $\text{Co}(\text{NO}_3)_2 \cdot 6\text{H}_2\text{O}$ (0.35 g, 1.2 mmol) in 30 mL of EtOH. The resulting orange solution was stirred for 2 min. after which 30% H_2O_2 (600 μL , 5.9 mmol) was added. The solution was filtered after stirring for 30 min. to afford a pink precipitate that was washed with EtOH (2 x 30 mL) followed by Et_2O (2 x 30 mL) and air dried. The product was dissolved in a minimum amount of hot H_2O (~ 2 mL) and crystallized overnight to afford X-ray quality crystals (0.43 g, 0.080 mmol, 76%). **${}^1\text{H}$ NMR** (d_2 -water, 300.13 MHz): δ 9.19 (d, $J_{\text{HH}} = 8.7$ Hz, 2H), 9.10 (d, $J_{\text{HH}} = 5.1$ Hz, 4H), 8.85 (d, $J_{\text{HH}} = 7.2$ Hz, 2H), 8.45 (m, 8H), 7.94 (t, $J_{\text{HH}} = 5.4$ Hz, 4H). **EA** Anal. Calcd (%) for $\text{C}_{30}\text{H}_{26}\text{Co}_2\text{F}_2\text{N}_{10}\text{O}_{16}$ (938.45): C, 38.40; H, 2.79; N, 14.93. Found: C, 38.10; H, 2.85; N, 14.51. **UV/Vis** (water, λ [nm] (ϵ [$\text{M}^{-1}\cdot\text{cm}^{-1} \div 10^3$])): 312 (11.8 ± 0.4), 324 (12.4 ± 0.4), 522 (0.30 ± 0.01).

Synthesis of $[\{\text{Co}_2(\mu\text{-OH})_2(\text{DPFN})\}_2(\kappa^2,\kappa^2\text{-PO}_4)][\text{NO}_3]_5 \cdot 15\text{ H}_2\text{O}$ (2). **1** (0.05 g, 0.05 mmol) was dissolved in 5 mL of water to which was added a solution of K_2HPO_4 (0.009 g, 0.05 mmol) and KOH (0.05 mL of 1M aq. soln) in 5 mL of water. The solution was stirred for 16 hr. after which the solvent was removed under vacuum. The red precipitate was dissolved in 10 mL of EtOH leaving undissolved a white powder. The solution was filtered and the solvent removed under vacuum after which the EtOH step was repeated. The product was dissolved in a minimum amount of water (~ 0.5 mL) and crystallized by vapor diffusion of acetonitrile into the aqueous

solution to afford a crude mixture containing a colorless solid and red X-ray quality crystals of **2** (0.026 g, 0.013 mmol, 52%). Impurities in the bulk sample were indicated by observation of complex multiplets at δ ca. 7.7 – 7.9, 8.2 – 8.5, 8.8 – 8.9, and 9.2 – 9.4 in the ^1H NMR spectrum. EA Anal. Calcd (%) for $\text{C}_{60}\text{H}_{44}\text{Co}_4\text{F}_4\text{N}_{17}\text{O}_{38}$ (1984.04): C, 36.32; H, 3.76; N, 12.00. Found: C, 36.91; H, 3.53; N, 11.10.

2. X-ray Crystallography Details

X-ray diffraction data were collected using Bruker AXS three-circle diffractometers coupled to a CCD detector with graphite-monochromated Mo K α ($\lambda = 0.71073 \text{ \AA}$) or Cu K α ($\lambda = 1.5478 \text{ \AA}$) radiation cooled under a stream of N_2 to 100 K. Raw data were integrated and corrected for Lorentz and polarization effects using Bruker APEX2 v. 2009.1. Absorption corrections were applied using SADABS. The structures were solved by direct methods using SHELXS and refined against F^2 on all data by full-matrix least squares with SHELXL-97. Refinement details for all compounds are detailed below:

DPMN

All non-hydrogen atoms were refined anisotropically; hydrogen atoms were included into the model at their geometrically calculated positions and refined using a riding model.

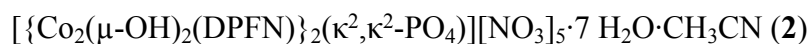
DPFN

All non-hydrogen atoms were refined anisotropically; hydrogen atoms were included into the model at their geometrically calculated positions and refined using a riding model.

$[\text{Co}_2(\mu\text{-OH})_2(\text{OH}_2)_2(\text{DPFN})][\text{NO}_3]_4$ (**1**)

All non-hydrogen atoms were refined anisotropically; hydrogen atoms were included into the model at their geometrically calculated positions and refined using a riding model except

hydrogen atoms of the aquo and hydroxo ligands, which were located from the electron difference map.



All non-hydrogen atoms were refined anisotropically; hydrogen atoms were included into the model at their geometrically calculated positions and refined using a riding model except hydrogen atoms of the water solvate molecules and hydroxo ligands, which were located from the electron difference map if possible or excluded when not possible. Two nitrate anions were located on an inversion center or mirror plane and were modeled as disordered over two symmetry-related sites with appropriate structure occupancy factors. One nitrate anion was located on a mirror plane and was modeled as disordered over two symmetry-related sites and one additional rotated site with a total structure occupancy factor of 1. For the site with the lowest occupancy, one nitrogen-oxygen bond length was restrained to a chemically appropriate value due to disorder. One nitrate anion was disordered over two sites and was modeled with half occupancy of each site. Due to disorder, bond lengths were restrained to chemically appropriate values, one site was restrained to be coplanar, and the anisotropic displacement parameters of the two sites were restrained to be similar. Two water solvate molecules were found to have partial occupancy and were modeled with 0.5 structural occupancy factors. For four water solvate molecule sites, hydrogen atoms could not be located from the electron difference map and were omitted from the model. For other water solvate molecules hydrogen bond lengths and angles were restrained to chemically appropriate values and isotropic displacement parameters were constrained to 1.5 times the isotropic value of the parent oxygen atom. For hydroxyl ligand hydrogen atoms, bond lengths were restrained to chemically appropriate values.

Table S1. Experimental details for the X-ray crystal structures of DPMN, DPFN, **1**, **2**.

	DPMN	DPFN	1	2
Chemical formula	C ₃₀ H ₂₂ N ₆	C ₃₀ H ₂₀ F ₂ N ₆	C ₃₀ H ₂₆ Co ₂ F ₂ N ₁₀ O ₁₆	C ₆₂ H ₆₁ Co ₄ F ₄ N ₁₈ O ₃₀ P
Formula Mass	466.54	502.52	938.47	1880.96
Crystal system	Triclinic	Monoclinic	Monoclinic	Monoclinic
a/Å	8.072(2)	8.7660(5)	26.800(2)	16.5997(17)
b/Å	12.076(3)	23.8721(16)	10.8131(8)	12.8750(14)
c/Å	12.881(3)	11.4381(7)	12.7351(10)	18.2563(19)
α/°	69.775(4)	90.00	90.00	90.00
β/°	84.874(4)	96.074(4)	106.8370(10)	112.203(2)
γ/°	79.297(4)	90.00	90.00	90.00
Unit cell volume/Å ³	1157.3(5)	2380.1(3)	3532.3(5)	3612.4(7)
Temperature/K	131(2)	100(2)	100(2)	100(2)
Space group	PError!	P2(1)/c	C2/c	P2(1)/m
No. of formula units per unit cell, Z	2	4	4	2
No. of reflections measured	4230	11151	3207	50251
No. of independent reflections	4230	3941	3207	6842
R _{int}	0.0281	0.0302	0.0313	0.0456
Final R ₁ values ($I > 2\sigma(I)$)	0.0353	0.0360	0.0245	0.0739
Final wR(F^2) values ($I > 2\sigma(I)$)	0.0820	0.0934	0.0680	0.2159
Final R ₁ values (all data)	0.0499	0.0419	0.0256	0.0907
Final wR(F^2) values (all data)	0.0889	0.0976	0.0692	0.2403
Goodness of fit on F^2	1.243	1.041	1.091	1.034

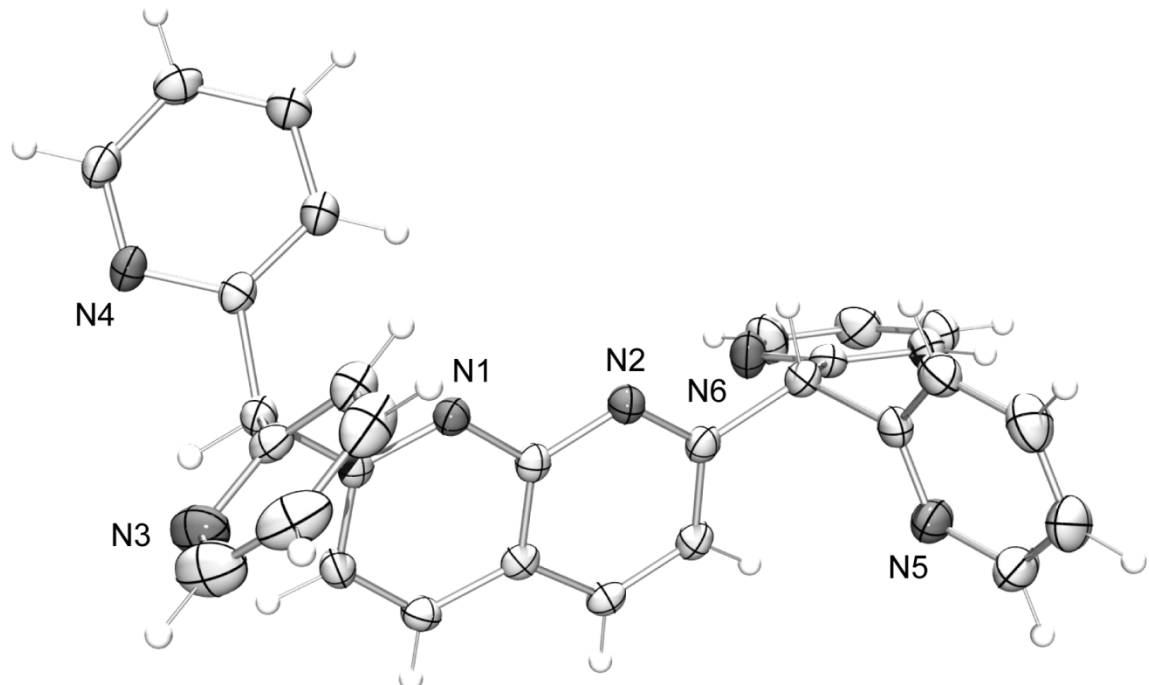


Figure S1. Crystal structure of DPMN.

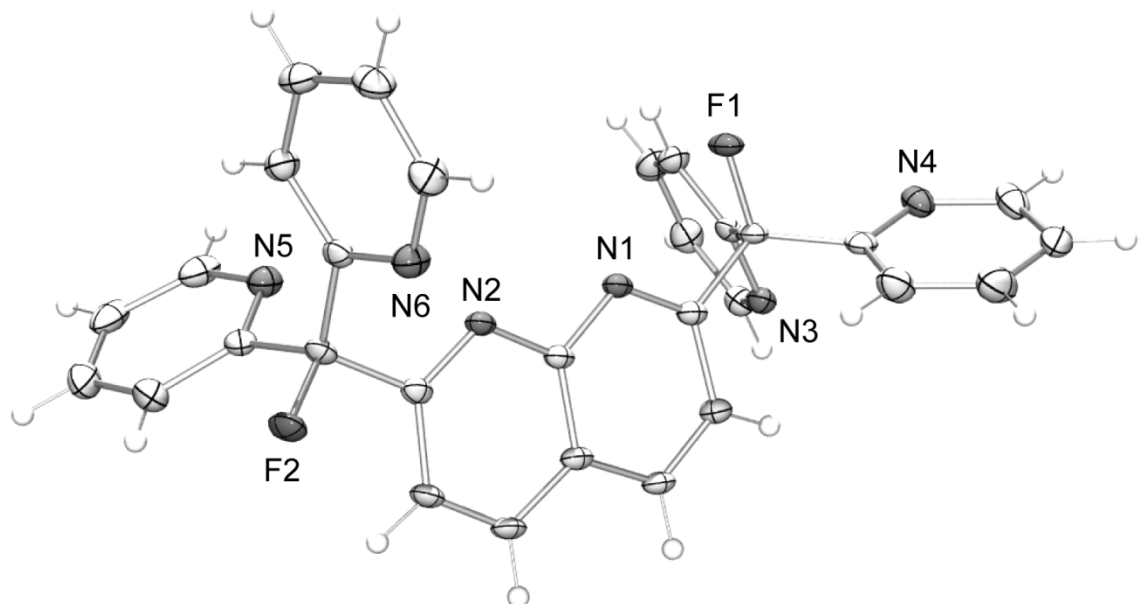


Figure S2. Crystal structure of DPFN.

3. Computational Details

DFT calculations were performed at the Molecular Graphics and Computation Facility of the University of California, Berkeley using the Gaussian 09 suite of *ab initio* programs.² Atoms were modeled using the meta generalized gradient approximation functional M06,³ and all-electron 6-31G** basis sets for all atoms.⁴ This functional/basis set combination was compared with combinations of the ωB97xD,⁵ TPSS,⁶ and B3LYP⁷ functionals with the cc-PVDZ (C,H,N,O)⁸ / cc-PVTZ⁹ (Co) and STO-3G¹⁰ basis sets as the closest match metrically of the optimized computational structure to the crystal structure of **1**. The DFT structures were optimized as gas phase structures using unrestricted wavefunctions. Protonation and oxidation states for species other than **1** were created by modification of **1** using Gaussview and optimized. Ground states were confirmed by comparison with optimized higher-spin analogues up to the high-spin limit for two high-spin cobalt centers. The 3D molecular structure figures displayed were drawn using the Gaussview and Adobe Illustrator visualization and manipulation programs. Molecular orbital surfaces were exported from Gaussview as cubefiles, visualized in VMD¹¹ and rendered with the Pov-Ray raytracer program.

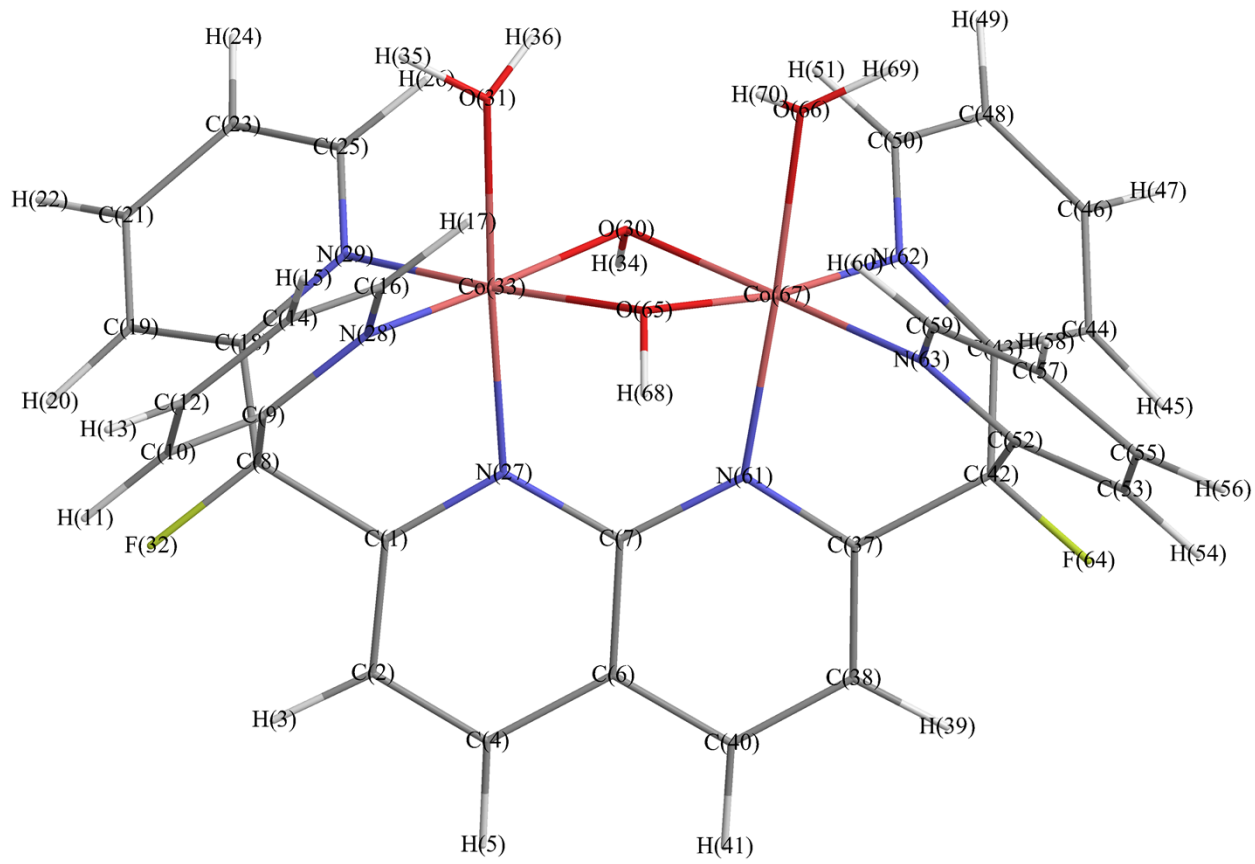


Figure S3. Optimized atomic coordinates of **1**. Selected bond lengths [\AA] and angles [$^{\circ}$]: Co(33)–Co(67) 2.838, Co(33)–O(30) 1.889, Co(33)–O(65) 1.899, Co(33)–O(31) 1.965, Co(33)–N(27) 1.938, Co(33)–N(28) 1.929, Co(33)–N(29) 1.937, Co(33)–O(30)–Co(67) 97.03.

Table S2. Cartesian coordinates of the optimized geometry of **1**.

	X (\AA)	Y (\AA)	Z (\AA)
C(1)	16.615069	-0.143157	-2.570082
C(2)	16.67754	-1.538555	-2.579198
H(3)	17.622359	-2.037709	-2.394563
C(4)	15.522082	-2.233131	-2.814959
H(5)	15.512088	-3.32167	-2.823519
C(6)	14.322186	-1.529824	-3.0473
C(7)	14.322185	-0.106391	-3.047297
C(8)	17.893558	0.633552	-2.257126
C(9)	18.261894	1.53613	-3.416951
C(10)	19.468689	1.441736	-4.085973
H(11)	20.200015	0.694617	-3.793587
C(12)	19.714456	2.332495	-5.129598
H(13)	20.655469	2.291377	-5.672821
C(14)	18.743909	3.271297	-5.467334
H(15)	18.902046	3.979598	-6.275156
C(16)	17.557196	3.300237	-4.753819
H(17)	16.769103	4.011428	-4.984764
C(18)	17.687443	1.4361	-0.985956
C(19)	18.474374	1.259792	0.138045

H(20)	19.282291	0.534954	0.130498
C(21)	18.203349	2.036476	1.262722
H(22)	18.806876	1.929865	2.160739
C(23)	17.14877	2.943754	1.222322
H(24)	16.899978	3.558047	2.082654
C(25)	16.406557	3.060415	0.059492
H(26)	15.566917	3.747216	0.000128
N(27)	15.497109	0.566995	-2.797304
N(28)	17.324045	2.444658	-3.736286
N(29)	16.676541	2.322267	-1.036764
O(30)	14.027152	2.714739	-1.848227
O(31)	15.822299	4.451084	-2.618902
F(32)	18.895787	-0.254632	-2.058754
Co(33)	15.697971	2.492262	-2.700306
H(34)	13.832665	2.095625	-1.129705
H(35)	16.676533	4.88372	-2.458456
H(36)	15.17187	4.851814	-2.020559
C(37)	12.029301	-0.143156	-3.524508
C(38)	11.966831	-1.538555	-3.515397
H(39)	11.022012	-2.037709	-3.700032
C(40)	13.12229	-2.233131	-3.279642
H(41)	13.132285	-3.32167	-3.271088
C(42)	10.75081	0.633552	-3.837459
C(43)	10.382476	1.53613	-2.677634
C(44)	9.175683	1.441734	-2.008609
H(45)	8.444358	0.694614	-2.300992
C(46)	8.929917	2.332494	-0.964984
H(47)	7.988905	2.291376	-0.421759
C(48)	9.900462	3.271299	-0.627253
H(49)	9.742326	3.979601	0.180568
C(50)	11.087174	3.30024	-1.34077
H(51)	11.875267	4.011433	-1.109828
C(52)	10.956923	1.4361	-5.10863
C(53)	10.169991	1.259791	-6.232629
H(54)	9.362073	0.534954	-6.225081
C(55)	10.441014	2.036476	-7.357307
H(56)	9.837485	1.929864	-8.255324
C(57)	11.495592	2.943754	-7.316909
H(58)	11.744382	3.558048	-8.177241
C(59)	12.237807	3.060415	-6.15408
H(60)	13.077446	3.747218	-6.094718
N(61)	13.14726	0.566995	-3.297285
N(62)	11.320325	2.44466	-2.358303
N(63)	11.967826	2.322266	-5.057824
F(64)	9.74858	-0.254631	-4.035829
O(65)	14.617216	2.71474	-4.246362
O(66)	12.822072	4.451086	-3.475689
Co(67)	12.946397	2.492264	-3.394284
H(68)	14.811704	2.095629	-4.964887
H(69)	11.96784	4.883727	-3.636127
H(70)	13.4725	4.851814	-4.074035

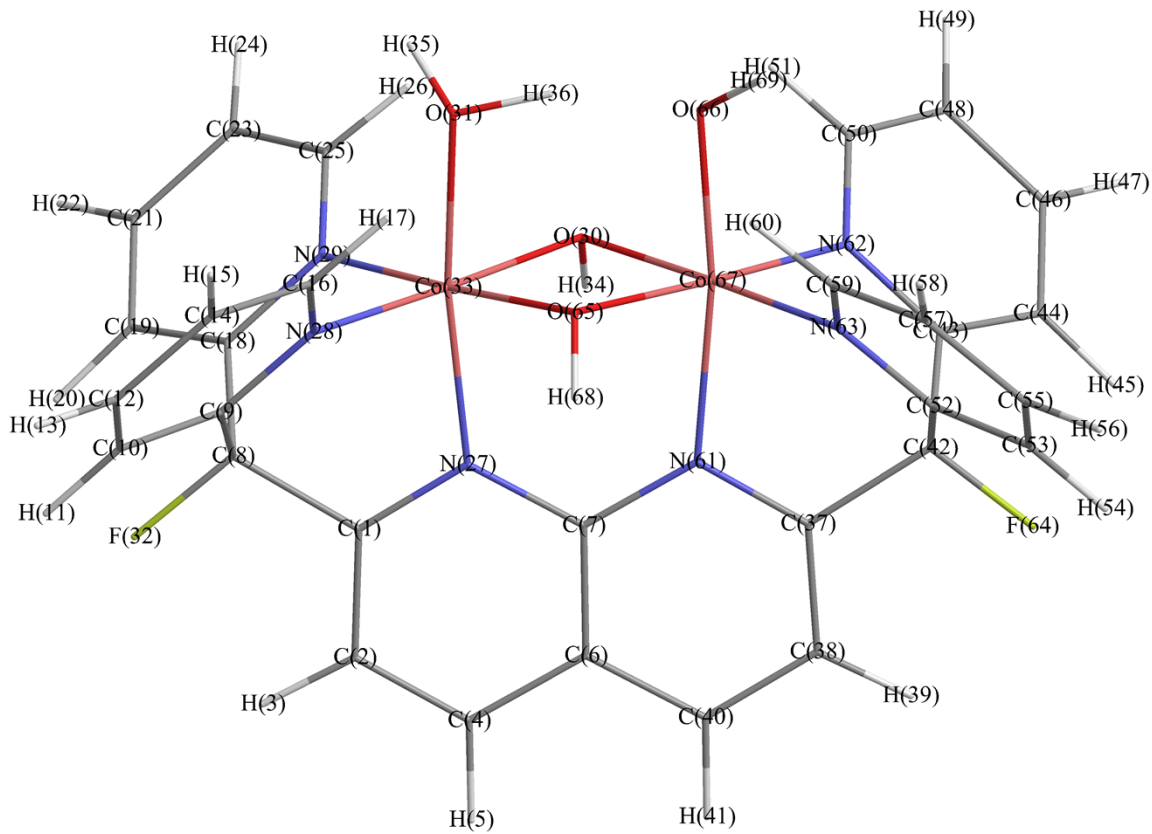


Figure S4. Optimized atomic coordinates of $[\text{Co}^{\text{III}}(\text{OH}_2)\text{Co}^{\text{III}}(\text{OH})]$. Selected bond lengths [\AA] and angles [$^\circ$]: Co(33)–Co(67) 2.754, Co(33)–O(30) 1.877, Co(33)–O(65) 1.875, Co(33)–O(31) 1.927, Co(33)–N(27) 1.946, Co(33)–N(28) 1.929, Co(33)–N(29) 1.932, Co(67)–O(30) 1.898, Co(67)–O(65) 1.898, Co(67)–O(66) 1.845, Co(67)–N(61) 1.992, Co(67)–N(62) 1.918, Co(67)–N(63) 1.921, Co(33)–O(30)–Co(67) 93.71, Co(33)–O(65)–Co(67) 93.76.

Table S3. Cartesian coordinates of the optimized geometry of $[\text{Co}^{\text{III}}(\text{OH}_2)\text{Co}^{\text{III}}(\text{OH})]$.

	X (\AA)	Y (\AA)	Z (\AA)
C(1)	16.62951	-0.196406	-2.524568
C(2)	16.68826	-1.595028	-2.519001
H(3)	17.62837	-2.093269	-2.312255
C(4)	15.53717	-2.289819	-2.778633
H(5)	15.52912	-3.377833	-2.783954
C(6)	14.3407	-1.590628	-3.043312
C(7)	14.34526	-0.170799	-3.040651
C(8)	17.89517	0.6066	-2.227867
C(9)	18.26188	1.482483	-3.411852
C(10)	19.47163	1.378368	-4.071909
H(11)	20.20008	0.63399	-3.768311
C(12)	19.7224	2.261475	-5.120607
H(13)	20.66502	2.2129	-5.658993
C(14)	18.76178	3.204462	-5.464418
H(15)	18.92938	3.912043	-6.270033
C(16)	17.57042	3.244504	-4.756244
H(17)	16.78935	3.965918	-4.971638

C(18)	17.69036	1.459018	-0.986314
C(19)	18.4761	1.324973	0.144009
H(20)	19.27605	0.592632	0.168221
C(21)	18.21164	2.154283	1.231219
H(22)	18.81522	2.082676	2.131915
C(23)	17.16589	3.067407	1.153673
H(24)	16.92423	3.720371	1.986278
C(25)	16.42042	3.136459	-0.011776
H(26)	15.57201	3.808483	-0.111766
N(27)	15.51834	0.502617	-2.772841
N(28)	17.33051	2.390277	-3.74692
N(29)	16.68981	2.35138	-1.069997
O(30)	14.07763	2.572004	-1.78259
O(31)	15.63572	4.363461	-2.836104
F(32)	18.90715	-0.269762	-1.99617
Co(33)	15.69553	2.440124	-2.724774
H(34)	13.91661	1.839126	-1.173419
H(35)	15.93306	4.913745	-2.100514
H(36)	14.64482	4.565174	-3.027684
C(37)	12.07028	-0.167747	-3.554646
C(38)	11.99262	-1.567365	-3.5676
H(39)	11.04689	-2.054006	-3.776458
C(40)	13.13514	-2.275725	-3.31164
H(41)	13.13241	-3.36372	-3.311314
C(42)	10.81843	0.657721	-3.847271
C(43)	10.4598	1.53775	-2.662238
C(44)	9.255212	1.43334	-1.992471
H(45)	8.529621	0.680467	-2.281367
C(46)	9.004615	2.330574	-0.955578
H(47)	8.066361	2.281602	-0.409734
C(48)	9.955485	3.29224	-0.637759
H(49)	9.78209	4.01553	0.152527
C(50)	11.14125	3.333943	-1.355847
H(51)	11.9136	4.077548	-1.186337
C(52)	11.03109	1.513603	-5.086986
C(53)	10.2531	1.374849	-6.22218
H(54)	9.462267	0.633107	-6.254222
C(55)	10.51003	2.214549	-7.303217
H(56)	9.911657	2.138854	-8.20697
C(57)	11.53641	3.147561	-7.21267
H(58)	11.76538	3.815821	-8.036589
C(59)	12.27476	3.222535	-6.042716
H(60)	13.0947	3.925231	-5.922501
N(61)	13.18726	0.516697	-3.303836
N(62)	11.3842	2.458522	-2.344788
N(63)	12.01918	2.420027	-4.994929
F(64)	9.7938	-0.205143	-4.081489
O(65)	14.66598	2.568937	-4.286602
O(66)	13.09761	4.340873	-3.247393
Co(67)	13.01454	2.500496	-3.353309
H(68)	14.80083	1.83751	-4.903756
H(69)	12.61193	4.827282	-3.922779

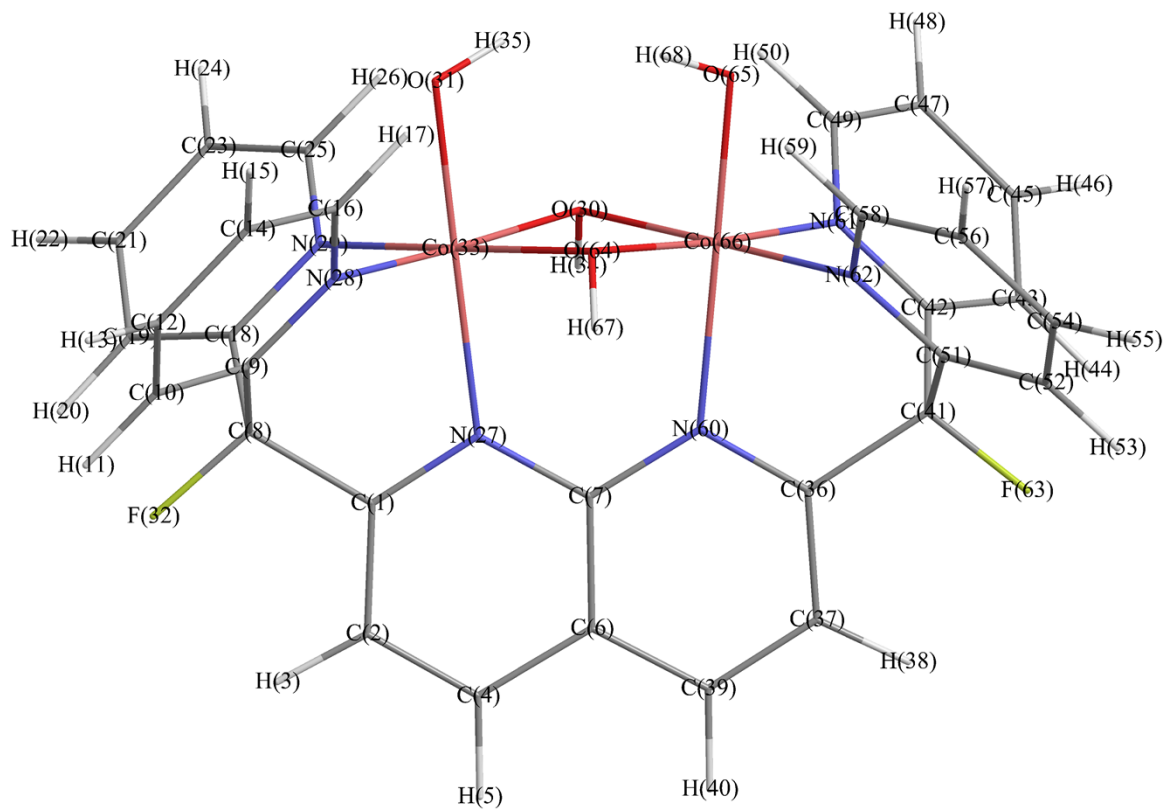


Figure S5. Optimized atomic coordinates of $[\text{Co}^{\text{III}}(\text{OH})]_2$. Selected bond lengths [\AA] and angles [$^\circ$]: Co(33)–Co(66) 2.792, Co(33)–O(30) 1.886, Co(33)–O(64) 1.901, Co(33)–O(31) 1.812, Co(33)–N(27) 2.037, Co(33)–N(28) 1.919, Co(33)–N(29) 1.928, Co(33)–O(30)–Co(66) 95.01.

Table S4. Cartesian coordinates of the optimized geometry of $[\text{Co}^{\text{III}}(\text{OH})]_2$

	X (\AA)	Y (\AA)	Z (\AA)
C(1)	16.593202	-0.209922	-2.5585
C(2)	16.670968	-1.611736	-2.557813
H(3)	17.619326	-2.097535	-2.36349
C(4)	15.526889	-2.318644	-2.800488
H(5)	15.526869	-3.406317	-2.80535
C(6)	14.322184	-1.629327	-3.047295
C(7)	14.322185	-0.20878	-3.047295
C(8)	17.850399	0.596788	-2.252998
C(9)	18.222404	1.507601	-3.410427
C(10)	19.430165	1.415976	-4.077481
H(11)	20.144323	0.642696	-3.817093
C(12)	19.696004	2.355108	-5.07161
H(13)	20.635226	2.316965	-5.616253
C(14)	18.764135	3.347212	-5.345207
H(15)	18.95409	4.106212	-6.096901
C(16)	17.574853	3.372062	-4.63145
H(17)	16.811725	4.135411	-4.752456
C(18)	17.653706	1.424064	-0.992403
C(19)	18.450766	1.266502	0.126956
H(20)	19.228288	0.511121	0.143088

C(21)	18.23069	2.114205	1.209252
H(22)	18.839823	2.023849	2.104105
C(23)	17.240092	3.083253	1.126036
H(24)	17.055138	3.772225	1.943488
C(25)	16.486082	3.17872	-0.033721
H(26)	15.722829	3.935682	-0.175777
N(27)	15.479804	0.480363	-2.793159
N(28)	17.31403	2.449879	-3.694931
N(29)	16.684247	2.34733	-1.065592
O(30)	14.016098	2.661991	-1.815335
O(31)	15.839627	4.308805	-2.631678
F(32)	18.875013	-0.281672	-2.044319
Co(33)	15.674457	2.50559	-2.700008
H(34)	13.85076	1.946018	-1.188879
H(35)	14.989972	4.630837	-2.297853
C(36)	12.051167	-0.209922	-3.536091
C(37)	11.973401	-1.611736	-3.536778
H(38)	11.025043	-2.097535	-3.731101
C(39)	13.11748	-2.318643	-3.294102
H(40)	13.1175	-3.406317	-3.28924
C(41)	10.793969	0.596788	-3.841592
C(42)	10.421965	1.507598	-2.684162
C(43)	9.214204	1.415972	-2.017108
H(44)	8.500045	0.642694	-2.277497
C(45)	8.948366	2.355102	-1.022976
H(46)	8.009144	2.316959	-0.478333
C(47)	9.880236	3.347204	-0.749378
H(48)	9.690283	4.106202	0.002319
C(49)	11.069518	3.372054	-1.463135
H(50)	11.832646	4.135403	-1.342128
C(51)	10.990661	1.424066	-5.102187
C(52)	10.1936	1.266506	-6.221545
H(53)	9.416077	0.511126	-6.237677
C(54)	10.413676	2.114209	-7.30384
H(55)	9.804542	2.023856	-8.198692
C(56)	11.404276	3.083256	-7.220625
H(57)	11.589231	3.772228	-8.038076
C(58)	12.158286	3.178721	-6.060868
H(59)	12.921541	3.935682	-5.918813
N(60)	13.164565	0.480363	-3.301432
N(61)	11.330339	2.449874	-2.399657
N(62)	11.960121	2.347331	-5.028997
F(63)	9.769357	-0.281674	-4.050272
O(64)	14.62827	2.661997	-4.279254
O(65)	12.804738	4.308803	-3.462906
Co(66)	12.969912	2.505588	-3.394581
H(67)	14.793611	1.946027	-4.905712
H(68)	13.654387	4.630839	-3.796743

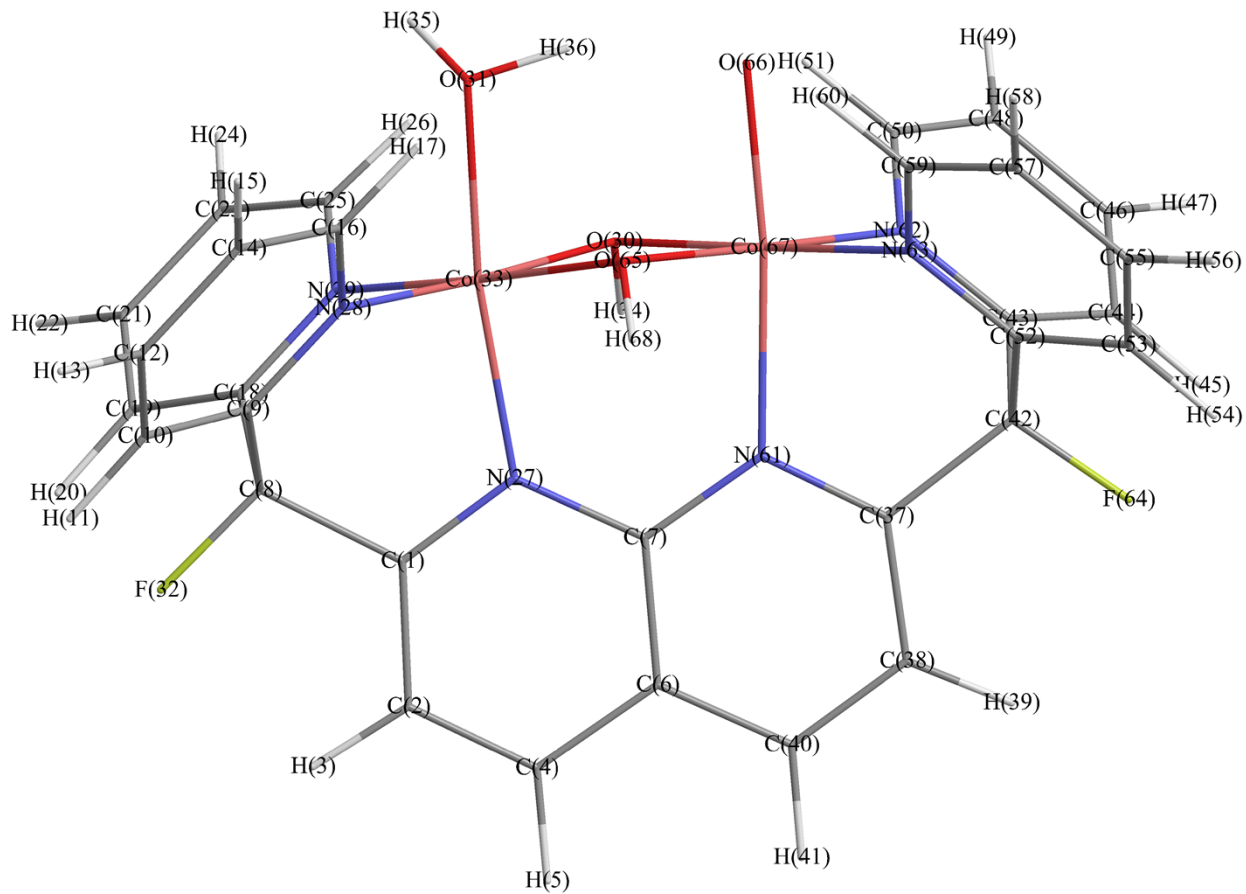


Figure S6. Optimized atomic coordinates of $[\text{Co}^{\text{III}}(\text{OH}_2)\text{Co}^{\text{IV}}(\text{O})]$. Selected bond lengths [\AA] and angles [$^\circ$]: Co(33)–Co(67) 2.762, Co(33)–O(30) 1.881, Co(33)–O(65) 1.876, Co(33)–O(31) 1.935, Co(33)–N(27) 1.945, Co(33)–N(28) 1.928, Co(33)–N(29) 1.933, Co(67)–O(30) 1.901, Co(67)–O(65) 1.897, Co(67)–O(66) 1.783, Co(67)–N(61) 2.008, Co(67)–N(62) 1.917, Co(67)–N(63) 1.916, Co(33)–O(30)–Co(67) 93.84, Co(33)–O(65)–Co(67) 94.15.

Table S5. Cartesian coordinates of the optimized geometry of $[\text{Co}^{\text{III}}(\text{OH}_2)\text{Co}^{\text{IV}}(\text{O})]$.

	X (\AA)	Y (\AA)	Z (\AA)
C(1)	16.636903	-0.200148	-2.50303
C(2)	16.703126	-1.597946	-2.491794
H(3)	17.645135	-2.089759	-2.278516
C(4)	15.558109	-2.301131	-2.756735
H(5)	15.557294	-3.3892	-2.759718
C(6)	14.360105	-1.609562	-3.031027
C(7)	14.355259	-0.189576	-3.030472
C(8)	17.900414	0.607282	-2.209155
C(9)	18.264029	1.473101	-3.400912
C(10)	19.474271	1.368467	-4.059749
H(11)	20.207879	0.633585	-3.745474
C(12)	19.71849	2.237568	-5.121648
H(13)	20.661523	2.18819	-5.659286
C(14)	18.749694	3.166407	-5.480927
H(15)	18.910391	3.861377	-6.298852

C(16)	17.558283	3.208365	-4.773058
H(17)	16.770768	3.917667	-5.004528
C(18)	17.692197	1.46778	-0.974754
C(19)	18.47788	1.346642	0.15708
H(20)	19.281391	0.618393	0.187292
C(21)	18.20872	2.182898	1.237717
H(22)	18.812037	2.121259	2.139384
C(23)	17.158767	3.090689	1.152111
H(24)	16.91354	3.749269	1.979271
C(25)	16.414137	3.147139	-0.014368
H(26)	15.56439	3.816309	-0.120395
N(27)	15.522636	0.49301	-2.758356
N(28)	17.325838	2.369227	-3.748763
N(29)	16.687374	2.354311	-1.066314
O(30)	14.07151	2.588516	-1.784866
O(31)	15.654761	4.360486	-2.841438
F(32)	18.91451	-0.264061	-1.969961
Co(33)	15.694175	2.429804	-2.722715
H(34)	13.900978	1.868774	-1.16218
H(35)	15.975774	4.931942	-2.131698
H(36)	14.686898	4.57397	-3.029216
C(37)	12.08518	-0.200439	-3.559005
C(38)	12.015751	-1.600774	-3.574319
H(39)	11.075089	-2.09352	-3.791459
C(40)	13.160504	-2.301864	-3.308942
H(41)	13.164622	-3.38988	-3.308444
C(42)	10.831538	0.617894	-3.856329
C(43)	10.460214	1.502388	-2.675438
C(44)	9.244857	1.402123	-2.023851
H(45)	8.52797	0.641593	-2.314388
C(46)	8.969306	2.313284	-1.006026
H(47)	8.020939	2.267003	-0.47771
C(48)	9.90726	3.287174	-0.685834
H(49)	9.714843	4.02339	0.087849
C(50)	11.104807	3.321378	-1.382465
H(51)	11.868114	4.070217	-1.190451
C(52)	11.028821	1.488951	-5.088381
C(53)	10.229883	1.377745	-6.210911
H(54)	9.458173	0.617019	-6.259592
C(55)	10.435438	2.278635	-7.254075
H(56)	9.819434	2.226612	-8.147627
C(57)	11.420109	3.251557	-7.133363
H(58)	11.59178	3.980578	-7.918715
C(59)	12.18532	3.295609	-5.978525
H(60)	12.958037	4.043753	-5.8229
N(61)	13.196192	0.489817	-3.299553
N(62)	11.37396	2.432342	-2.351905
N(63)	11.993758	2.417163	-4.981167
F(64)	9.812352	-0.250932	-4.09134
O(65)	14.659784	2.567197	-4.281225
O(66)	13.013863	4.270612	-3.366103
Co(67)	13.005925	2.48795	-3.355748
H(68)	14.789551	1.84944	-4.915446

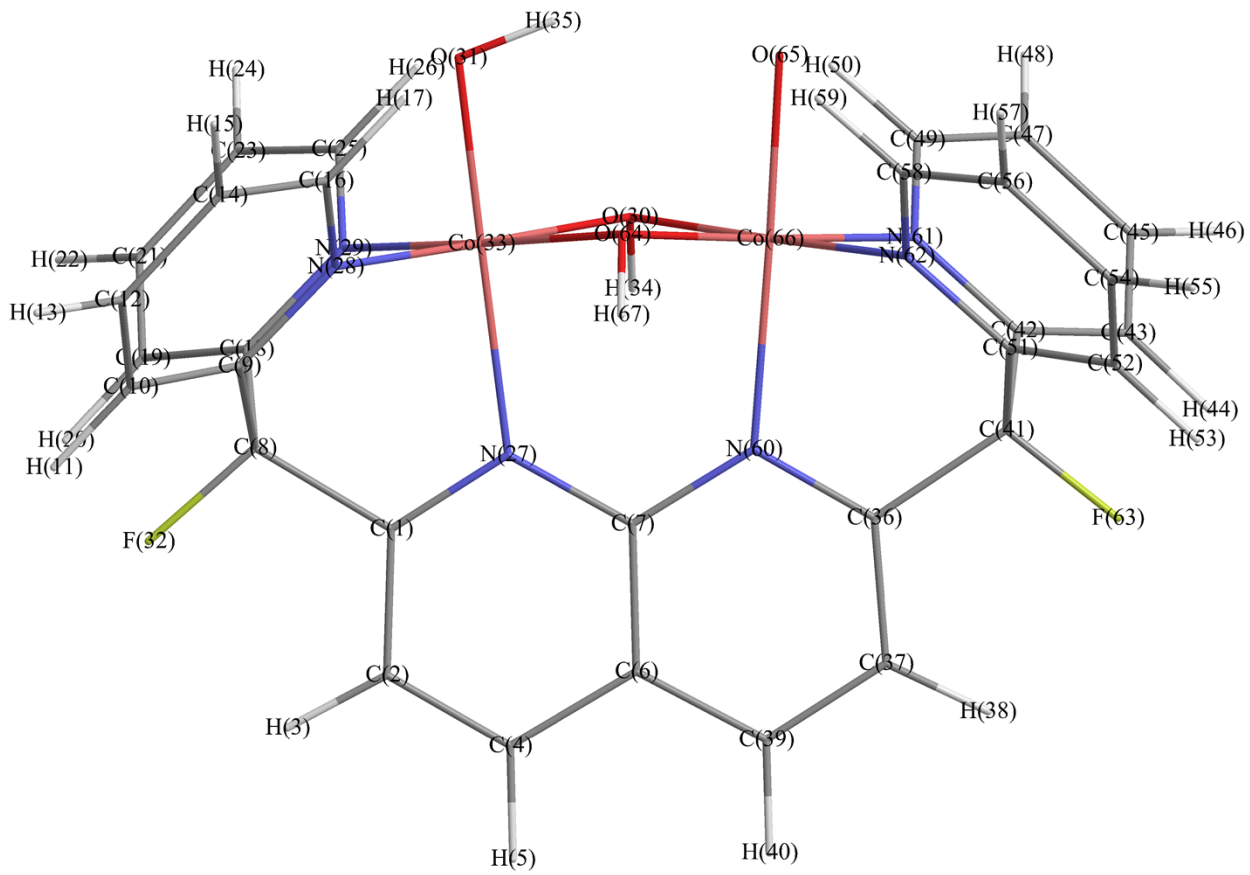


Figure S7. Optimized atomic coordinates of $[\text{Co}^{\text{III}}(\text{OH})\text{Co}^{\text{IV}}(\text{O})]$. Selected bond lengths [\AA] and angles [$^\circ$]: Co(33)–Co(66) 2.778, Co(33)–O(30) 1.900, Co(33)–O(64) 1.900, Co(33)–O(31) 1.802, Co(33)–N(27) 2.049, Co(33)–N(28) 1.919, Co(33)–N(29) 1.920, Co(66)–O(30) 1.887, Co(66)–O(64) 1.887, Co(66)–O(65) 1.769, Co(66)–N(60) 2.034, Co(66)–N(61) 1.921, Co(66)–N(62) 1.922, Co(33)–O(30)–Co(66) 94.37, Co(33)–O(64)–Co(66) 94.39.

Table S6. Cartesian coordinates of the optimized geometry of $[\text{Co}^{\text{III}}(\text{OH})\text{Co}^{\text{IV}}(\text{O})]$.

	X (\AA)	Y (\AA)	Z (\AA)
C(1)	16.593202	-0.209922	-2.5585
C(2)	16.670968	-1.611736	-2.557813
H(3)	17.619326	-2.097535	-2.36349
C(4)	15.526889	-2.318644	-2.800488
H(5)	15.526869	-3.406317	-2.80535
C(6)	14.322184	-1.629327	-3.047295
C(7)	14.322185	-0.20878	-3.047295
C(8)	17.850399	0.596788	-2.252998
C(9)	18.222404	1.507601	-3.410427
C(10)	19.430165	1.415976	-4.077481
H(11)	20.144323	0.642696	-3.817093
C(12)	19.696004	2.355108	-5.07161
H(13)	20.635226	2.316965	-5.616253
C(14)	18.764135	3.347212	-5.345207
H(15)	18.95409	4.106212	-6.096901
C(16)	17.574853	3.372062	-4.63145

H(17)	16.811725	4.135411	-4.752456
C(18)	17.653706	1.424064	-0.992403
C(19)	18.450766	1.266502	0.126956
H(20)	19.228288	0.511121	0.143088
C(21)	18.23069	2.114205	1.209252
H(22)	18.839823	2.023849	2.104105
C(23)	17.240092	3.083253	1.126036
H(24)	17.055138	3.772225	1.943488
C(25)	16.486082	3.17872	-0.033721
H(26)	15.722829	3.935682	-0.175777
N(27)	15.479804	0.480363	-2.793159
N(28)	17.31403	2.449879	-3.694931
N(29)	16.684247	2.34733	-1.065592
O(30)	14.016098	2.661991	-1.815335
O(31)	15.839627	4.308805	-2.631678
F(32)	18.875013	-0.281672	-2.044319
Co(33)	15.674457	2.50559	-2.700008
H(34)	13.85076	1.946018	-1.188879
H(35)	14.989972	4.630837	-2.297853
C(36)	12.051167	-0.209922	-3.536091
C(37)	11.973401	-1.611736	-3.536778
H(38)	11.025043	-2.097535	-3.731101
C(39)	13.11748	-2.318643	-3.294102
H(40)	13.1175	-3.406317	-3.28924
C(41)	10.793969	0.596788	-3.841592
C(42)	10.421965	1.507598	-2.684162
C(43)	9.214204	1.415972	-2.017108
H(44)	8.500045	0.642694	-2.277497
C(45)	8.948366	2.355102	-1.022976
H(46)	8.009144	2.316959	-0.478333
C(47)	9.880236	3.347204	-0.749378
H(48)	9.690283	4.106202	0.002319
C(49)	11.069518	3.372054	-1.463135
H(50)	11.832646	4.135403	-1.342128
C(51)	10.990661	1.424066	-5.102187
C(52)	10.1936	1.266506	-6.221545
H(53)	9.416077	0.511126	-6.237677
C(54)	10.413676	2.114209	-7.30384
H(55)	9.804542	2.023856	-8.198692
C(56)	11.404276	3.083256	-7.220625
H(57)	11.589231	3.772228	-8.038076
C(58)	12.158286	3.178721	-6.060868
H(59)	12.921541	3.935682	-5.918813
N(60)	13.164565	0.480363	-3.301432
N(61)	11.330339	2.449874	-2.399657
N(62)	11.960121	2.347331	-5.028997
F(63)	9.769357	-0.281674	-4.050272
O(64)	14.62827	2.661997	-4.279254
O(65)	12.804738	4.308803	-3.462906
Co(66)	12.969912	2.505588	-3.394581
H(67)	14.793611	1.946027	-4.905712
H(68)	13.654387	4.630839	-3.796743

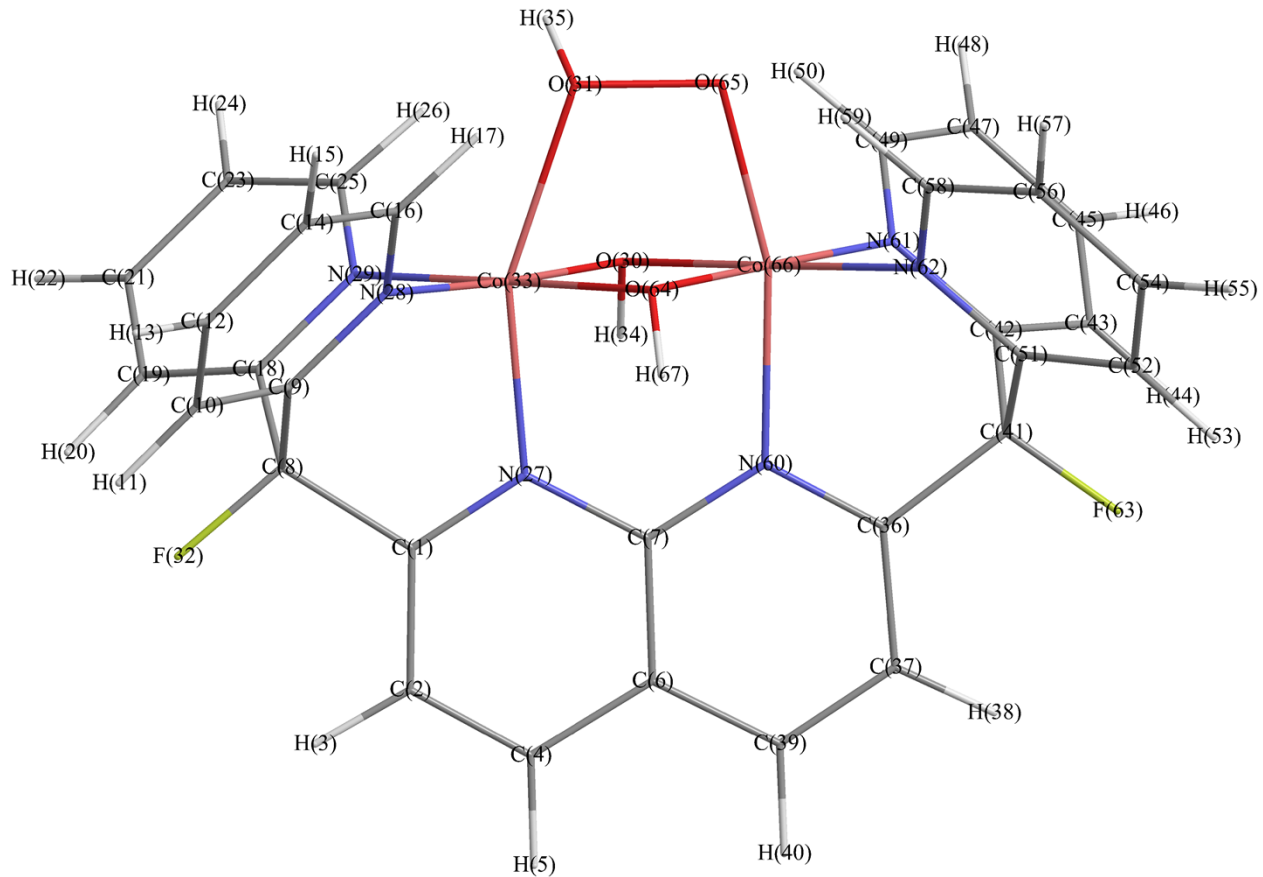


Figure S8. Optimized atomic coordinates of $[\text{Co}^{\text{III}}]_2(\mu\text{-OOH})$. Selected bond lengths [\AA] and angles [$^\circ$]: Co(33)–Co(66) 2.589, Co(33)–O(30) 1.864, Co(33)–O(64) 1.862, Co(33)–O(31) 2.063, Co(33)–N(27) 1.925, Co(33)–N(28) 1.917, Co(33)–N(29) 1.935, Co(66)–O(30) 1.886, Co(66)–O(64) 1.879, Co(66)–O(65) 1.877, Co(66)–N(60) 1.969, Co(66)–N(61) 1.916, Co(66)–N(62) 1.913, Co(33)–O(30)–Co(66) 87.33, Co(33)–O(64)–Co(66) 87.60.

Table S7. Cartesian coordinates of the optimized geometry of $[\text{Co}^{\text{III}}]_2(\mu\text{-OOH})$.

	X (\AA)	Y (\AA)	Z (\AA)
C(1)	16.641944	-0.266471	-2.501682
C(2)	16.702751	-1.666446	-2.485778
H(3)	17.644742	-2.163915	-2.282541
C(4)	15.549156	-2.36785	-2.733873
H(5)	15.550449	-3.456078	-2.729821
C(6)	14.342546	-1.681408	-3.003945
C(7)	14.345814	-0.265827	-3.00678
C(8)	17.880162	0.588381	-2.233316
C(9)	18.203086	1.487167	-3.419949
C(10)	19.407409	1.425738	-4.094338
H(11)	20.151297	0.684782	-3.820862
C(12)	19.634064	2.348532	-5.115243
H(13)	20.571983	2.332034	-5.663783
C(14)	18.658654	3.290566	-5.417952
H(15)	18.811508	4.029578	-6.197979
C(16)	17.468865	3.283102	-4.70529

H(17)	16.665971	3.989012	-4.898516
C(18)	17.667906	1.459914	-1.001152
C(19)	18.482045	1.370437	0.112662
H(20)	19.28872	0.645577	0.141582
C(21)	18.241464	2.237509	1.176585
H(22)	18.869012	2.200869	2.062951
C(23)	17.192214	3.145007	1.092652
H(24)	16.973615	3.832049	1.903892
C(25)	16.412478	3.164026	-0.052493
H(26)	15.559155	3.828982	-0.148208
N(27)	15.520294	0.409607	-2.741826
N(28)	17.254639	2.39004	-3.725042
N(29)	16.655093	2.341851	-1.086878
O(30)	14.062946	2.36292	-1.702105
O(31)	14.958627	4.264629	-3.001276
F(32)	18.926383	-0.247673	-2.012231
Co(33)	15.622113	2.331435	-2.722619
H(34)	13.912007	1.58331	-1.151732
H(35)	14.967346	4.863456	-2.234789
C(36)	12.068049	-0.24403	-3.544981
C(37)	11.988018	-1.645346	-3.553183
H(38)	11.045536	-2.135218	-3.772014
C(39)	13.128736	-2.356632	-3.280295
H(40)	13.117128	-3.444738	-3.276591
C(41)	10.85558	0.633792	-3.851623
C(42)	10.51585	1.543936	-2.674448
C(43)	9.295709	1.488066	-2.027545
H(44)	8.559292	0.743357	-2.310437
C(45)	9.039809	2.423169	-1.025319
H(46)	8.087898	2.410581	-0.501493
C(47)	10.001741	3.375823	-0.714743
H(48)	9.824627	4.128895	0.046351
C(49)	11.20672	3.363473	-1.401091
H(50)	11.996414	4.085318	-1.218733
C(51)	11.102843	1.509957	-5.077058
C(52)	10.323011	1.432447	-6.214921
H(53)	9.535761	0.690096	-6.291386
C(54)	10.566705	2.345149	-7.241202
H(55)	9.965704	2.316857	-8.146056
C(56)	11.567416	3.296385	-7.090381
H(57)	11.765958	4.032039	-7.863129
C(58)	12.317703	3.306969	-5.923558
H(59)	13.106606	4.029013	-5.732882
N(60)	13.188939	0.418955	-3.279417
N(61)	11.454098	2.45528	-2.356932
N(62)	12.085242	2.419966	-4.94436
F(63)	9.801123	-0.187082	-4.096071
O(64)	14.6894	2.312415	-4.333728
O(65)	13.522016	4.215922	-3.277706
Co(66)	13.105312	2.385869	-3.326539
H(67)	14.800257	1.515563	-4.868077

Table S8. Optimized Spin States for Computational Structures

	\hat{S}^2
1	0
[Co ^{III} (OH ₂)Co ^{III} (OH)]	0
[Co ^{III} (OH)] ₂	0
[Co ^{III} (OH ₂)Co ^{IV} (O)]	0.7501
[Co ^{III} (OH)Co ^{IV} (O)]	0.7501
[Co ^{III}] ₂ (μ-OOH)	0

4. Electrochemical Details

Electrochemical experiments were recorded with a BASi Epsilon potentiostat using a 3 mm diameter glassy carbon working electrode, a Pt wire counter electrode. For aqueous experiments, a [Ag]/[AgCl] reference electrode (sat. KCl, 0.197 V vs. NHE) was used. The glassy carbon working electrode was polished between runs with an alumina slurry and rinsed with water. Phosphate buffered solutions were made using 0.1 M H₃PO₄, 0.1 M KH₂PO₄, or 0.1 M K₂HPO₄ in Milli-Q water and the pH was adjusted using aliquots of a 1 M KOH solution. Borate buffered solutions were made using 0.025 M Na₂B₄O₇ in Milli-Q water and the pH was adjusted using aliquots of a 1 M NaOH solution. Cyclic voltammetry and differential pulse voltammetry experiments were conducted with an analyte concentration of 2 mM. The potentials of redox events were measured as the potential at peak current from a differential pulse voltammogram. For DPFN, the cyclic voltammogram was collected with a 2mM analyte concentration in a solution of 0.1 M [^tBu₄N][PF₆] in dimethylformamide and referenced to ferrocene/ferrocinium as an internal standard. Controlled potential electrolysis (CPE) experiments were conducted in pH 9.0 aqueous phosphate buffer solution or borate buffer solution with an analyte concentration of 1 mM for a period of 10 min at 1.6 V.

Oxygen detection experiments were carried out in a sealed two-cell setup such that the headspace above the working and reference electrodes was separate from the headspace above

the counter electrode and the cell solutions were connected by glass frit in which CPE was conducted for a period of 4 hr at 1.6 V in pH 9.0 aqueous phosphate buffer solution using a 16.2 cm² ITO working electrode with an analyte concentration of 0.2 mM. Oxygen was detected using an Ocean Optics Multi-Frequency Phase Fluorimeter with a FOSPOR-R sensor located in the headspace of the working electrode cell.

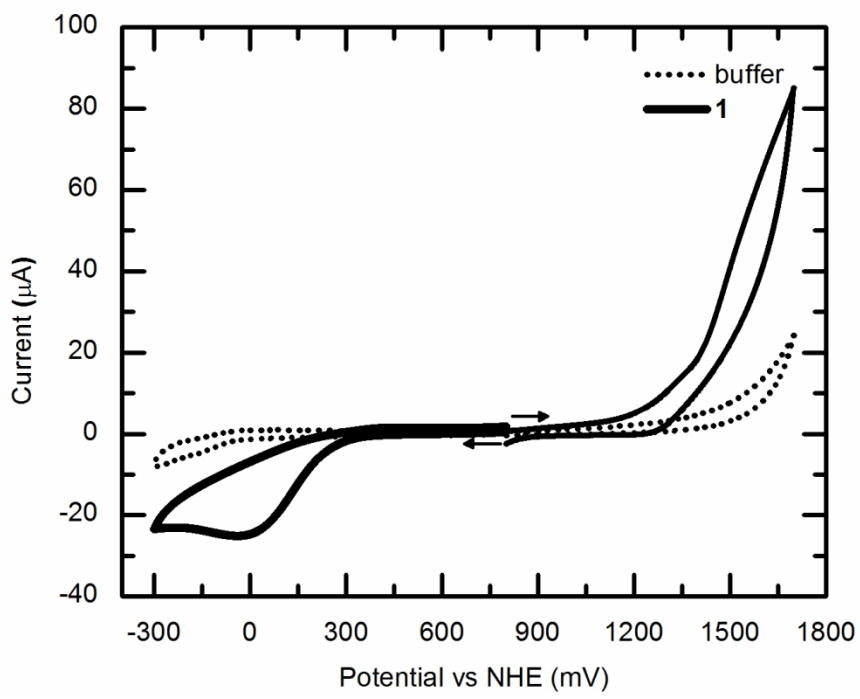


Figure S9. Cyclic voltammograms of 2 mM **1** at pH 9.0 in 0.1 M KP_i aqueous buffer solution and buffer only. Scanning rate is 100 mV/s and potentials are reported relative to the normal hydrogen electrode.

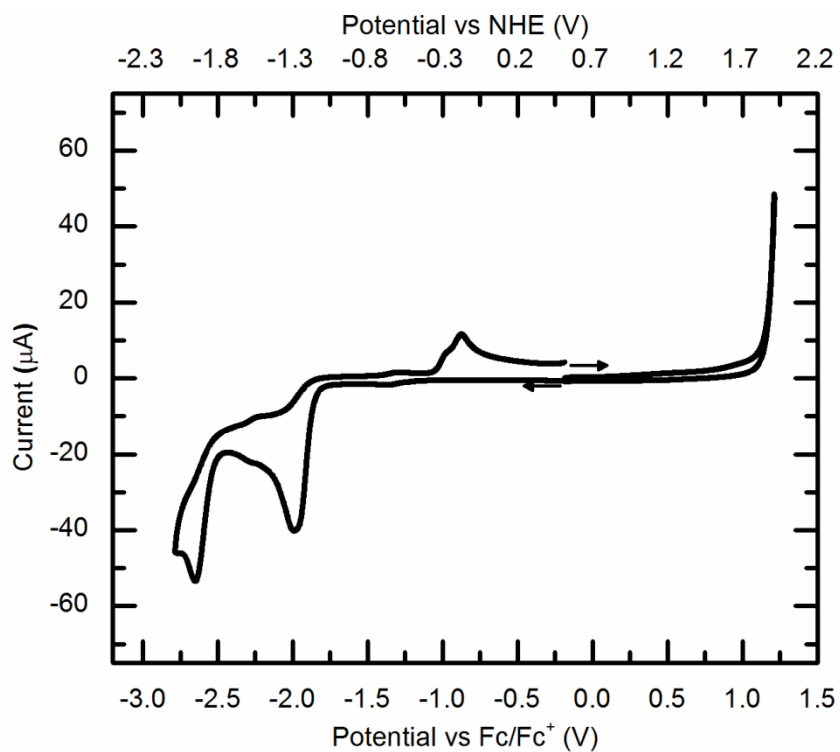


Figure S10. Cyclic voltammogram of 2 mM DPFN in 0.1 M $t\text{Bu}_4\text{NPF}_6$ DMF solution referenced to Fc/Fc^+ in a separate experiment. Scanning rate is 100 mV/s. Potentials vs. NHE are taken as Fc/Fc^+ (DMF) = 0.72 V vs. NHE.¹²

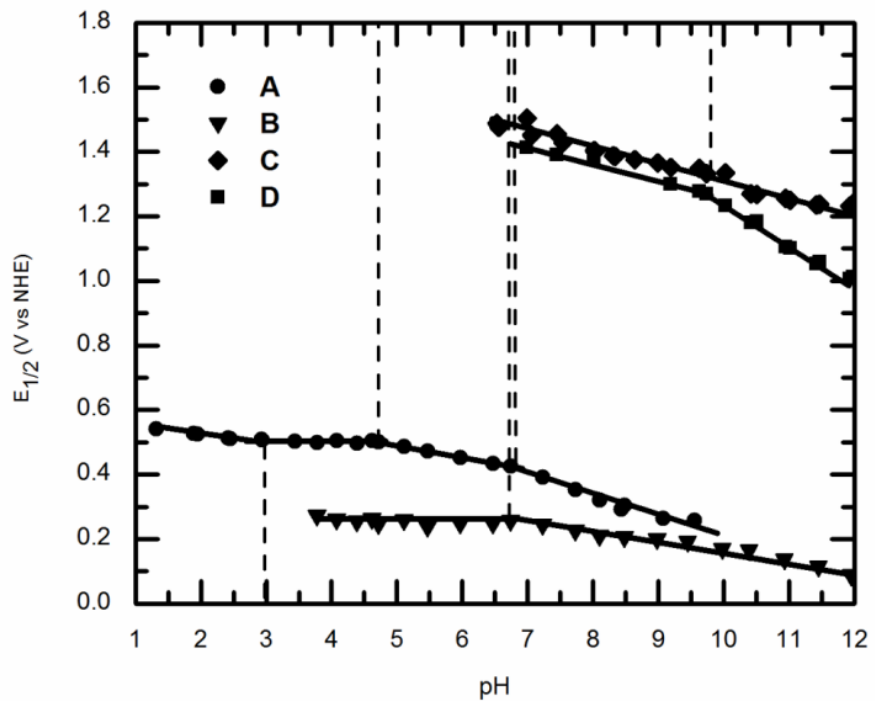


Figure S11. Pourbaix diagram of **1** in phosphate buffer solution from pH 1–12 in the potential window 0–1.8 V vs. NHE. Potentials of electrochemical events are determined by differential pulse voltammetry; (●) A, (▼) B, (◆) C, (■) D.

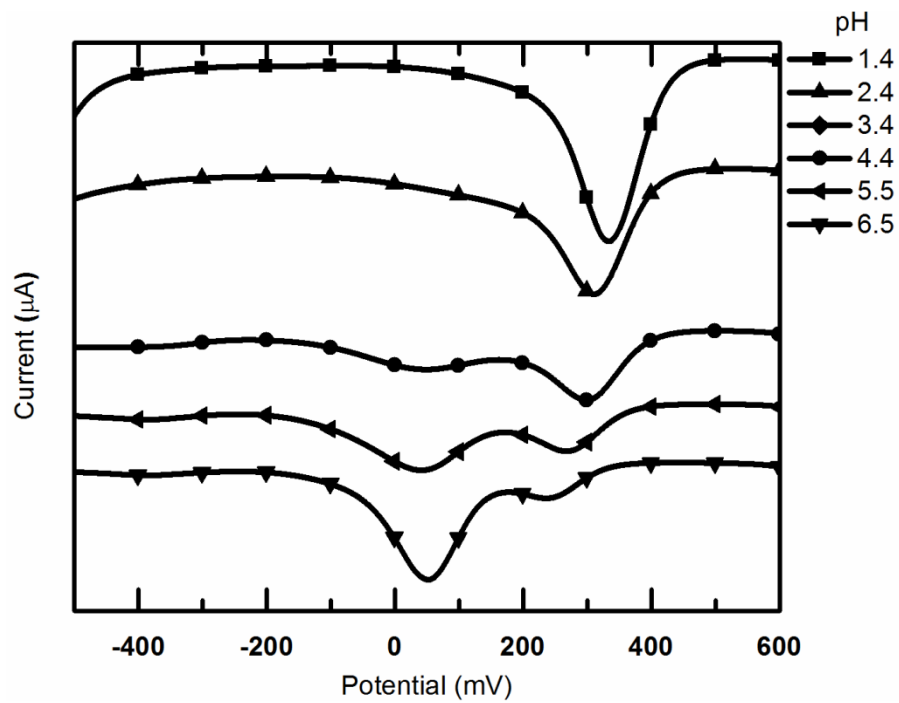


Figure S12. Cathodic differential pulse voltammograms of **1** with variation of pH from 1.4–6.5.

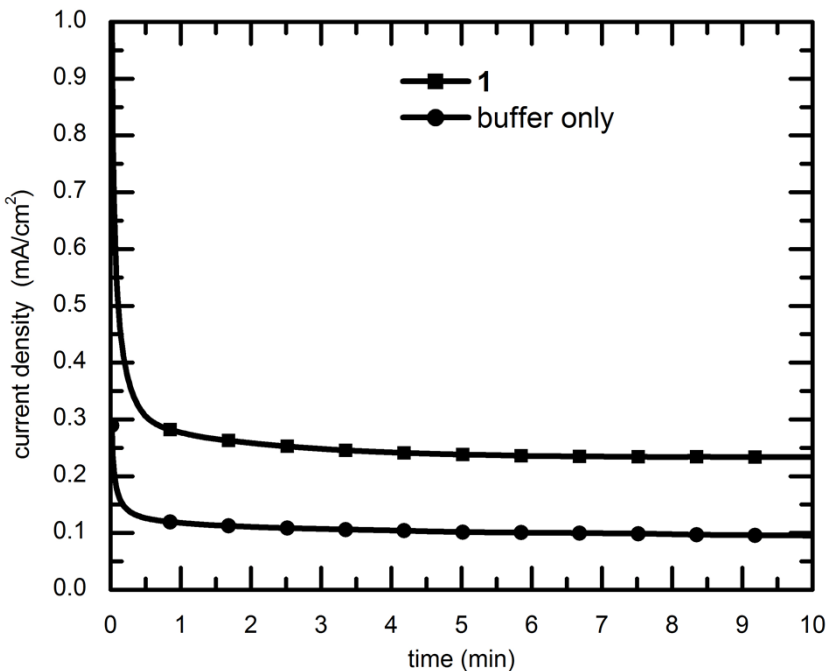


Figure S13. Controlled potential electrolysis of **1** at 1.6 V in phosphate buffer solution at pH 9.0, (■) **1**, (●) buffer only. The electrode was pretreated by holding at 1.6 V for 10 min in phosphate buffer solution at pH 9.0.

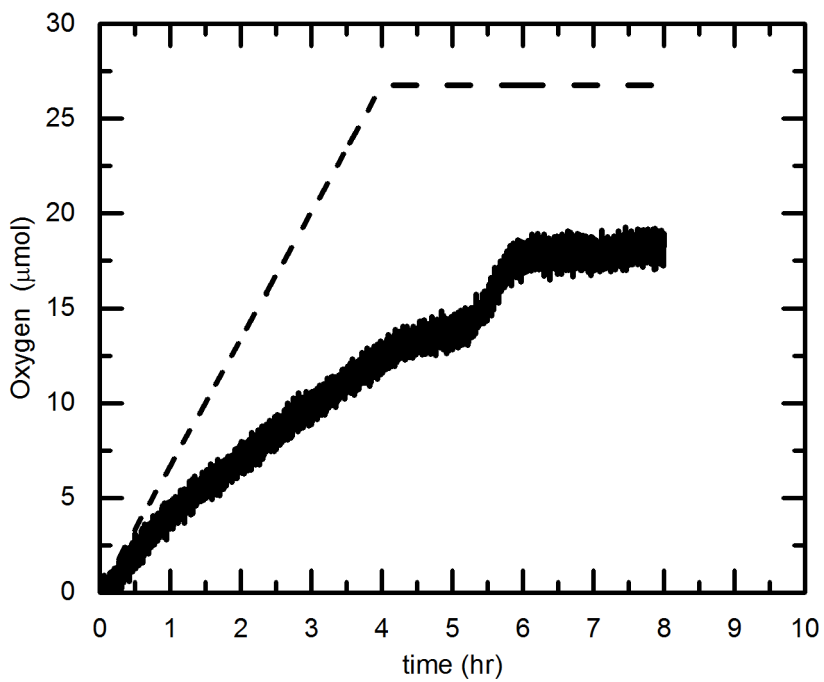


Figure S14. Evolved oxygen detection during controlled potential electrolysis of **1** at 1.6 V in phosphate buffered solution at pH 9. Dashed line represents expected oxygen evolution at 100% faradaic efficiency after correction for background current in phosphate buffer only.

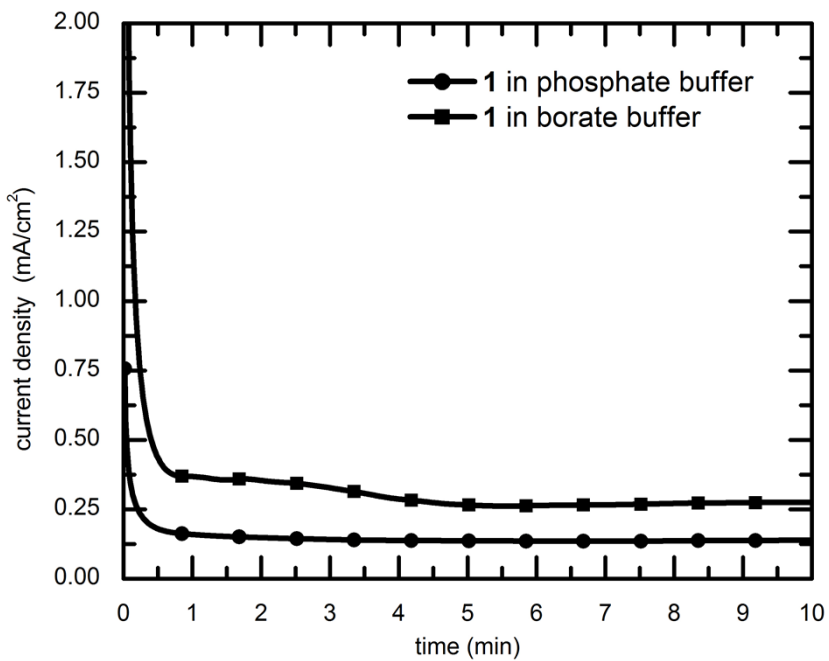


Figure S15. Comparison of background-subtracted controlled potential electrolysis of **1** at 1.6 V in phosphate and borate buffer solutions at pH 9, (●) phosphate buffer, (■) borate buffer.

5. References

1. G. R. Newkome, S. J. Garbis, V. K. Majestic, F. R. Fronczek, and G. Chiari, *J. Org. Chem.*, 1981, **46**, 833–839.
2. Gaussian 09, Revision A.1, M. J. Frisch, G. W. Trucks, H. B. Schlegel, G. E. Scuseria, M. A. Robb, J. R. Cheeseman, G. Scalmani, V. Barone, B. Mennucci, G. A. Petersson, H. Nakatsuji, M. Caricato, X. Li, H. P. Hratchian, A. F. Izmaylov, J. Bloino, G. Zheng, J. L. Sonnenberg, M. Hada, M. Ehara, K. Toyota, R. Fukuda, J. Hasegawa, M. Ishida, T. Nakajima, Y. Honda, O. Kitao, H. Nakai, T. Vreven, J. A. Montgomery, Jr., J. E. Peralta, F. Ogliaro, M. Bearpark, J. J. Heyd, E. Brothers, K. N. Kudin, V. N. Staroverov, R. Kobayashi, J. Normand, K. Raghavachari, A. Rendell, J. C. Burant, S. S. Iyengar, J. Tomasi, M. Cossi, N. Rega, J. M. Millam, M. Klene, J. E. Knox, J. B. Cross, V. Bakken, C. Adamo, J. Jaramillo, R. Gomperts, R. E. Stratmann, O. Yazyev, A. J. Austin, R. Cammi, C. Pomelli, J. W. Ochterski, R. L. Martin, K. Morokuma, V. G. Zakrzewski, G. A. Voth, P. Salvador, J. J. Dannenberg, S. Dapprich, A. D. Daniels, Ö. Farkas, J. B. Foresman, J. V. Ortiz, J. Cioslowski, and D. J. Fox, Gaussian, Inc., Wallingford CT, (2009).
3. Y. Zhao and D. G. Truhlar, *Theor. Chem. Acc.*, 2007, **120**, 215–241.
4. P. C. Hariharan and J. A. Pople, *Theor. Chim. Acta*, 1973, **28**, 213–222.
5. J.-D. Chai and M. Head-Gordon, *Phys. Chem. Chem. Phys.*, 2008, **10**, 6615–6620.
6. J. Tao, J. P. Perdew, V. N. Staroverov, and G. E. Scuseria, *Phys. Rev. Lett.*, 2003, **91**, 146401.
7. A. D. Becke, *J. Chem. Phys.*, 1993, **98**, 5648–5652.
8. T. H. Dunning, *J. Chem. Phys.*, 1989, **90**, 1007–1023.
9. R. A. Kendall, T. H. Dunning, and R. J. Harrison, *J. Chem. Phys.*, 1992, **96**, 6796–6806.
10. W. J. Hehre, R. F. Stewart, and J. A. Pople, *J. Chem. Phys.*, 1969, **51**, 2657–2664.
11. W. Humphrey, A. Dalke, and K. Schulten, *J. Mol. Graphics*, 1996, **14**, 33–38.
12. T. J. Smith and K. J. Stevenson, in *Handbook of Electrochemistry*, Elsevier, 2007, p. 101.